ResearchGate

See discussions, stats, and author profiles for this publication at: https://www.researchgate.net/publication/233790535

Optical absorption and fluorescence spectra of novel annulated analogues of azafluoranthene and azulene dyes

ARTICLE *in* MATERIALS CHEMISTRY AND PHYSICS · JUNE 2010

Impact Factor: 2.26 · DOI: 10.1016/j.matchemphys.2010.02.010

CITATIONS
17

READS
44

4 AUTHORS, INCLUDING:

Krzysztof S Danel
University of Agriculture in Krakow
40 PUBLICATIONS **527** CITATIONS
SEE PROFILE

Tomasz Uchacz
Jagiellonian University
26 PUBLICATIONS **170** CITATIONS
SEE PROFILE

Andriy V. Kityk
Czestochowa University of Technology
206 PUBLICATIONS **1,935** CITATIONS
SEE PROFILE

All in-text references underlined in blue are linked to publications on ResearchGate, letting you access and read them immediately.

Available from: Andriy V. Kityk
Retrieved on: 26 January 2016

Provided for non-commercial research and education use.
Not for reproduction, distribution or commercial use.

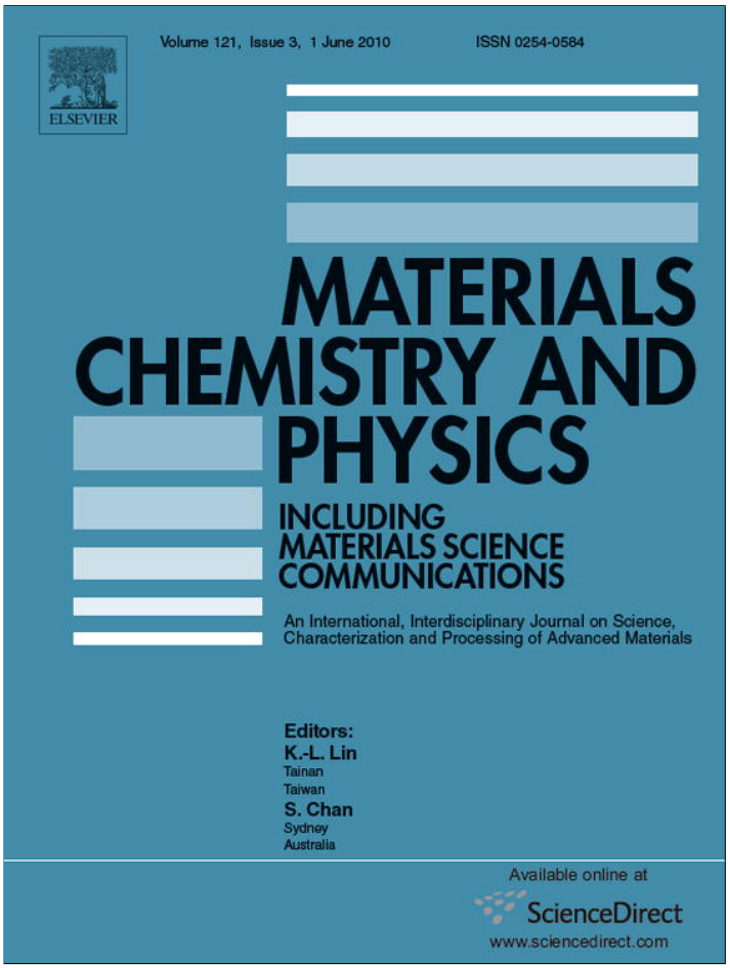

This article appeared in a journal published by Elsevier. The attached copy is furnished to the author for internal non-commercial research and education use, including for instruction at the authors institution and sharing with colleagues.

Other uses, including reproduction and distribution, or selling or licensing copies, or posting to personal, institutional or third party websites are prohibited.

In most cases authors are permitted to post their version of the article (e.g. in Word or Tex form) to their personal website or institutional repository. Authors requiring further information regarding Elsevier's archiving and manuscript policies are encouraged to visit:

http://www.elsevier.com/copyright

Author's personal copy

Materials Chemistry and Physics 121 (2010) 477–483

Contents lists available at ScienceDirect

Materials Chemistry and Physics

journal homepage: www.elsevier.com/locate/matchemphys

Optical absorption and fluorescence spectra of novel annulated analogues of azafluoranthene and azulene dyes

S. Całus [a], K.S. Danel [b], T. Uchacz [c], A.V. Kityk [a,*]

[a] Faculty of Electrical Engineering, Częstochowa University of Technology, Al. Armii Krajowej 17, 42-200 Częstochowa, Poland
[b] Department of Chemistry, University of Agriculture, Balicka str. 122, 30-149 Kraków, Poland
[c] Faculty of Chemistry, Jagiellonian University, Ingardena str. 3, 30-060 Kraków, Poland

ARTICLE INFO

Article history:
Received 25 November 2009
Accepted 8 February 2010

Keywords:
Optical absorption spectra
Fluorescence spectra
Semiempirical calculations
Organic dyes

ABSTRACT

Paper reports optical absorption and fluorescence spectra as well as basic photophysical characteristics of newly synthesized 1,3-diphenyl-*3H*-indeno[1,2,3-*de*]pyrazolo[3,4-*b*]quinoline (DPIPQ) and 6-phenyl-*6H*-5,6,7-triazadibenzo[*f*,*h*]naphtho[3,2,1-*cd*]azulene (PTNA) dyes being recorded in organic solvents of different polarity. The experimental results are compared with the quantum chemical calculations performed within the semiempirical method PM3. While the solvent polarity changes from cyclohexane to acetonitrile both dyes exhibit the hypsochromic (blue) shift of the absorption spectra and the bathochromic (red) shift of the fluorescence spectra. This fact is found to be consistent with the Lippert–Mataga solvatochromic model and is explained by a specific orientation of the ground and excited state dipole moments. Quantitative evaluations of the solvatochromic shifts give quite well agreement with the experimental data only for optical absorption spectra of both dyes. In the case of the fluorescence spectra the experiment suggests much larger dipole moment of the excited state comparing to the one which follows from the semiempirical calculations. Corresponding discrepancy is especially strong for DPIPQ dye and is assumed to be related with an enhanced mixing of the lowest LE state with the lowest ICT states due to lowering of their energies in a polar solvent environment. Both dyes reveal substantial quantum yield thus may be considered as candidates for the luminescent or electroluminescent applications. Depending on solvent polarity they emit light in the green-yellow range of the visible spectra.

© 2010 Elsevier B.V. All rights reserved.

1. Introduction

The electronic structure and spectral properties of numerous low weight organic dyes attract much attention during the last decade in a context of their broad range of applications in optoelectronic and electroluminescent devices, such as dye lasers [1–3], organic light emitting diodes (OLEDs) and electroluminescence displays (ELDs) [4–6], photovoltaic devices [7], etc. The key area of the investigations usually lies in search of new organic materials that exhibit full color gamut, high efficiency and stability under normal conditions. In order to achieve high fluorescence quantum yields and tunable emission wavelengths or bandwidths, the origin of the light emission process has to be understood. Accordingly, the electronic states and transitions as well as their correlation with structural, environmental and chemical substitution effects appear in a scope of experimental and theoretical studies where the optical spectroscopy methods are usually combined with a quantum chemical analysis and/or modeling [8–12].

Actual work deals with newly synthesized dyes representing the derivatives of annulated analogues of azafluoranthene and azulene with chemical structures given as:

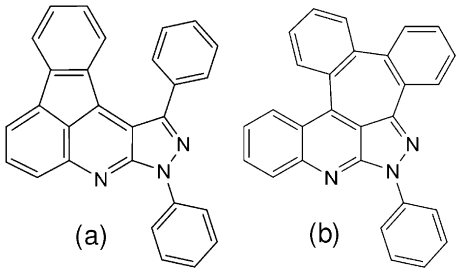

where the compound (**a**) is 1,3-diphenyl-*3H*-indeno[1,2,3-*de*]pyrazolo[3,4-*b*]quinoline (abbreviated hereafter as DPIPQ) and the compound (**b**) is 6-phenyl-*6H*-5,6,7-triazadibenzo[*f*,*h*]naphtho[3,2,1-*cd*]azulene (abbreviated hereafter as PTNA), respectively [13]. The azafluoranthene skeleton is also

* Corresponding author.
E-mail address: kityk@ap.univie.ac.at (A.V. Kityk).

0254-0584/$ – see front matter © 2010 Elsevier B.V. All rights reserved.
doi:10.1016/j.matchemphys.2010.02.010

Author's personal copy

present in alkaloids [14–17], and recently its potential as a candidate for OLEDs applications has been validated [18]. Pharmacologically, derivatives of azafluoranthenes are useful to enhance oxygenation of tissues and as antidepressant agents [19,20]. Also, azulene-based compounds have been exploited in organic light emitting devices and are considered as pharmacologically important compounds [21–23]. On the other hand, the structure PTNA is interesting because of nonplanar distortion of the aromatic rings imposed by steric hindrance of interacting hydrogen atoms. Similar ring arrangements are presented in carbon nanotubes as so-called Stone–Wales defects giving rise to different deformations of carbon nanotubes [24–29]. DPIPQ and PTNA dyes can be used for optoelectronic applications and they can possibly exert some biological effects binding to macromolecules, e.g. DNA. In addition, both compounds can be considered as potentially promising ligands of triplet emitters (phosphors) [30,31].

In the present paper we report the optical absorption and photoluminescent properties of DPIPQ and PTNA. The optical absorption and photoluminescence spectra of these dyes are recorded in cyclohexane (CHX), tetrahydrofuran (THF) or acetonitrile (ACN) representing weakly, medium or highly polar organic solvents, respectively. The goal of this study is to analyze the change of the electronic structure caused by solvent-modified electron transfer interactions. Accordingly, the experimental spectra are consequently subjected to the quantum chemical analysis performed in the framework of the semiempirical quantum chemical method PM3.

2. Synthesis

Routines concerning the synthesis of heterocycles dyes are presented in scheme below. The DPIPQ (**2**) and PTNA (**3**) compounds have been obtained performing the chemical reactions:

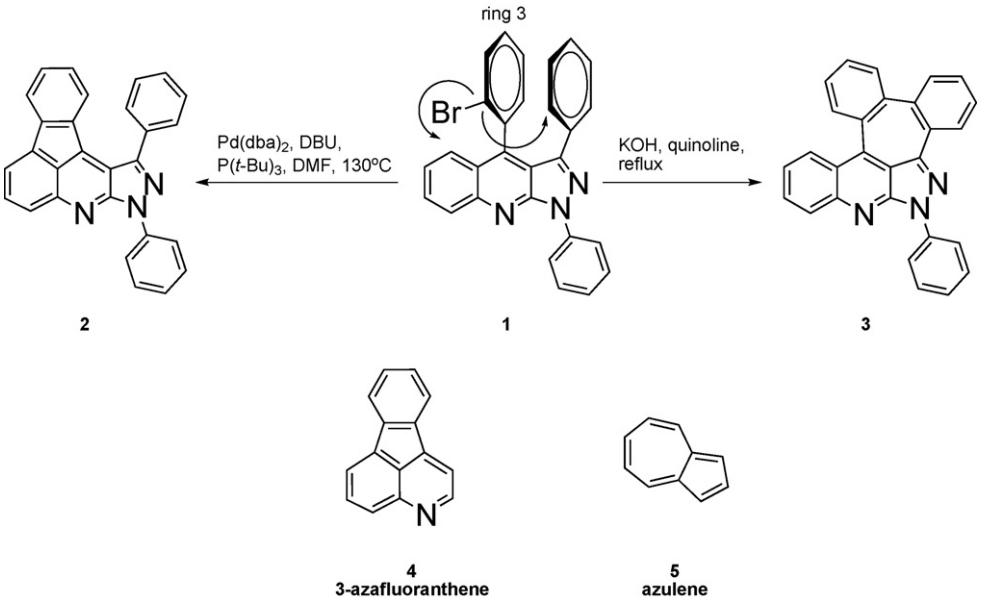

i.e. were synthesized from pyrazolo[3,4-b]quinolines **1**[13]. Looking at the structure of **1** it is easy to notice the proximity of the neighboring aromatic rings. Therefore it was tempting to hinder permanently the rotation of the *phenyl ring 3* by means of cyclization reactions. Depending on the reaction conditions it was easy to convert the readily accessible **1** to one of the desired regioisomers. It is worth to mention that the basic 3-azafluoranthene framework is prepared in many steps [17]. The synthesis of triazadibenzo[cd,g]azulenes has been reported recently in Ref. [32]. The obtained compounds **2** and **3** can be considered as annulated derivatives of 3-azafluoranthene **4** or heterocyclic analogues of azulene **5**.

Commercially available reagents (Aldrich, Fluka, Merck) were used without further purification. ^{1}H NMR and ^{13}C NMR were recorded using a Mercury-Vx 300 MHz Varian operating at 300 and 75 MHz, respectively, in $CDCl_3$ with tetramethylsilane (TMS) as an internal standard. Melting points were measured on a MELT-Temp and are uncorrected. The purity of the obtained compounds was checked by TLC. The mass spectra (ESI) were recorded on a Esquire 3000 Bruker Daltonics mass spectrometer (Brema, Germany). Elementary analyses were performed on a PerkinElmer 2400 CHN analyzer.

6-Phenyl-6H-5,6,7-triazadibenzo[f,h]naphtho[3,2,1-cd]azulene (**3**, PTNA). **1** (553 mg, 1.16 mmol), powdered KOH (1.95 g, 34.8 mmol) and quinoline (20 mL) were refluxed for 3–4 h until reaction was completed (TLC, toluene). After cooling, the orange solution was treated with 10% hydrochloric acid (100 mL) and extracted with toluene (2× 20 mL). The organic phase was washed with saturated aqueous NaCl solution, dried over anhydrous $MgSO_4$ and evaporated to dryness. The residue was dissolved in chloroform and MeOH was added dropwise on sonication in a cold water bath (1 h). Yellow solid was filtered off; yield, 307 mg (67%); mp = 203–205 °C; ^{1}H NMR (300 MHz, $CDCl_3$) δ 7.30 (t, 1H, J = 7.5 Hz), 7.38–7.53 (m, 5H), 7.58 (t, 2H, J = 7.5 Hz), 7.70–7.75 (m, 2H), 7.80–7.83 (m, 1H), 7.86 (dd, 1H, J = 8.1, 1.2 Hz), 8.16 (dd, 1H, J =8.4, 0.6 Hz), 8.31–8.34 (m, 1H), 8.44 (dd, 1H, J = 8.7, 0.9 Hz), 8.60 (d, 2H, J = 8.7 Hz); ^{13}C NMR (75 MHz, $CDCl_3$) δ 120.31, 120.95, 121.82, 123.69, 125.16, 127.45, 127.54, 127.61, 128.62, 128.88, 129.01, 129.11, 129.52, 129.98, 132.08, 133.47, 134.25, 134.64, 135.40, 138.17, 140.13, 140.68, 142.12, 143.70, 150.49, 150.65; MS (ESI): m/z 396 $(MH)^+$; Anal. calcd. for $C_{28}H_{17}N_3$; C, 85.04; H, 4.33; N, 10.63. Found: C, 84.92; H, 4.46; N, 10.61.

1,3-Diphenyl-3H-indeno[1,2,3-de]pyrazolo[3,4-b]quinoline (**2**, DPIPQ). **1** (476 mg, 1 mmol), $Pd_2(dba)_3$ (25 mg, 0.024 mmol, 2.4% mol) and DBU (0.30 mL) were placed in a 25 mL round-bottomed flask. The flask was capped with a rubber septum and dry DMF (15 mL) was added through a syringe. The mixture was flushed with argon for 30 min and P(t-Bu)$_3$ in toluene (19.4 mg, 0.096 mmol, 0.12 mL) was added in one portion. The mixture was stirred for another 10 min at room temperature then the yellow solution was stirred for 3 h in an oil bath at 130 ° C until starting material

Author's personal copy

disappeared. After cooling, the deep brown solution was poured into water (25 mL). The mixture was extracted with toluene (2× 25 mL). The organic phase was washed with saturated aqueous NaCl solution and dried over anhydrous $MgSO_4$. After evaporation, the residue was treated with chloroform (5 mL) and MeOH was added dropwise on sonication in a cold water bath. An orange precipitate was filtered off; yield 285 mg (72%); mp = 212–214 °C; ^{1}H NMR (300 MHz, $CDCl_3$) δ 6.90 (dt, 1H, J = 7.5, 0.6 Hz), 7.03 (td, 1H, J = 7.5, 1.2 Hz), 7.31 (dd, 1H, J = 7.5, 1.2 Hz), 7.34 (t, 1H, J = 7.2 Hz), 7.55–7.63 (m, 5H), 7.72 (dd, 2H, J = 4.8, 1.2 Hz), 7.75–7.83 (m, 3H), 7.95–8.00 (m, 1H), 8.53 (d, 2H, J = 8.7 Hz); ^{13}C NMR (75 MHz, $CDCl_3$) δ 112.81, 118.92, 121.61, 121.65, 123.98, 125.82, 127.72, 127.93, 128.27, 128.54, 129.01, 129.37, 129.90, 130.22, 132.30, 133.90, 137.35, 138.34, 139.82, 139.87, 140.98, 144.79, 145.90, 153.07; MS (ESI): m/z 396 $(MH)^+$. Anal. calcd. for $C_{28}H_{17}N_3$: C, 85.04; H, 4.33; N,10.63. Found: C, 85.11; H, 4.37; N, 10.48.

3. Experimental and calculation procedures

The optical absorption spectra were recorded in organic solutions with concentration of DPIPQ or PTNA dyes of about 10^{-5} M (it refers to absorbances of ca. 0.1 at excitation wavelength in the fluorescence). To probe the solvatochromic effect on the absorption spectra the measurements have been carried out using CHX, THF and ACN as solvents. The measurements were performed by means of Shimadzu UV-VIS 2101 scanning spectrophotometer in the range of 230–600 nm using a standard 1 cm path length quartz cuvette for absorption spectrometry.

The steady-state photoluminescence measurements were performed using a conventional spectrofluorimeter with cooled photomultiplier EMI 955 8B operating with a single photon counting mode. For excitation the 365 nm Hg line was selected. The fluorescence spectra were corrected for the spectral sensitivity of the detecting system. The samples (prepared in the darkness) were degassed before experiments using the freezing–pumping–thawing technique. The fluorescence quantum yields were determined from the steady-state measurements using the corrected for spectral sensitivity fluorescence spectra of quinine sulphate in 0.05 M H_2SO_4 ($\Phi_{fl} = 0.53$) [33], as an actinometer. The fluorescence lifetimes were estimated from the decay curves measured by time-resolved single photon counting. As an excitation source a picosecond diode laser ($\lambda = 400$ nm, $\tau = 70$ ps pulse duration) from IBH-UK was used.

The absorption spectra were calculated according to procedure described in [34–36]. The geometrical optimization as well as the calculations of excitation energies, excited-state and transition dipole moments have been performed by means of the commercial computation program HyperChem-8.0 using the semiempirical quantum chemical method PM3. The electronic transitions were calculated taking into account only the singly excited configuration interactions (CI) applying the orbital criterion with 24 occupied and 24 unoccupied orbitals. The empirical parameter Γ, describing Gaussian band broadening, has been adjusted in each case in order to reproduce actual bandwidth of measured absorption bands.

4. Results and discussion

The conformational search has been performed within the semiempirical method PM3 for the isolated molecules in vacuo ($T = 0$ K) in their ground state. Both dyes are characterized by several equilibrium molecular geometries with the same or nearly the same total energies. Fig. 1(a) and (b) shows only one of those equilibrium states for DPIPQ and PTNA dyes, respectively. Other equilibrium molecular geometries differ from each other by angular orientations of their phenyl moieties characterizing by twist

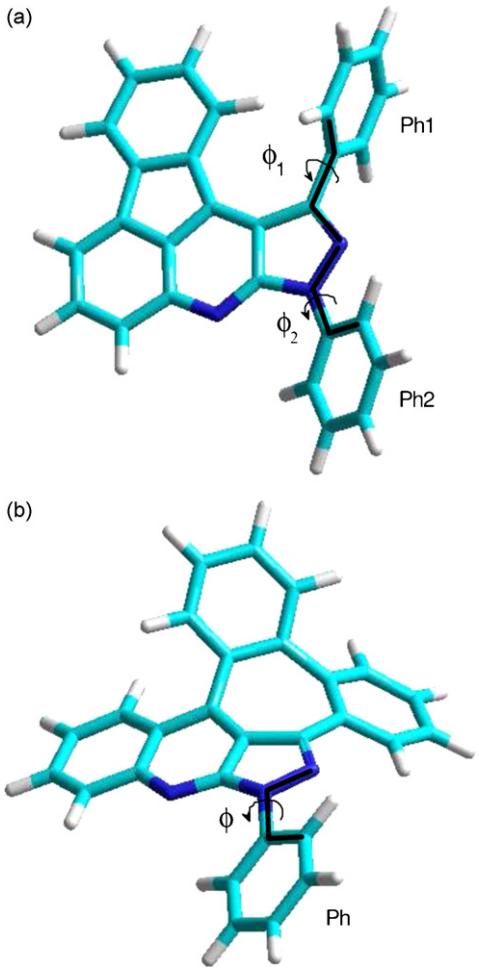

Fig. 1. The equilibrium molecular conformations of DPIPQ [(a)] and PTNA [(b)] dyes as obtained within the semiempirical quantum chemical method PM3. ϕ_1, ϕ_2 or ϕ are the torsion angles defining the angular orientation of the phenyl rings Ph1, Ph2 or Ph, respectively.

potential with two equilibrium angular positions. We describe these positions by the torsion angles ϕ (as for PTNA) and ϕ_1 or ϕ_2 (as for DPIPQ), see Fig. 1. PTNA exhibits the equilibrium twist angles at $\phi(1) \approx -15°$ and $\phi(2) \approx 45°$ related with the asymmetric twist potential ($E[\phi(2)] - E[\phi(1)] \approx 0.006$ eV) and separated by small angular energy barrier $\Delta E \approx 0.007$–0.013 eV. It is evident, that the asymmetry of the potential energy for PTNA dye appears as a direct sequence of specific geometry of phenyl-azulene moiety having substantially bent shape in the ground state. Contrary to this, the phenyl-azafluoranthene moiety is perfectly flat in the ground state of the DPIPQ molecule. Accordingly, the equilibrium twist angles $\phi_2(1) \approx 22°$ and $\phi_2(2) \approx -22°$ are bounded to a symmetric potential and are separated by the energy barrier ΔE of 0.027 eV. The equilibrium angular orientation of the Ph1 group only slightly deviates from the orthogonal one [see Fig. 1(a)] due to a weak interaction between the phenyl moieties Ph2 and Ph1. More precisely, the equilibrium angles ϕ_1 and ϕ_2 correlate each other thus two slightly non-orthogonal equilibrium positions of the Ph1 group at $\phi_1(1) \approx 86°$ or $\phi_1(2) \approx 94°$ are bonded to the equilibrium angular positions of Ph2 group at $\phi_2 = \phi_2(2)$ or $\phi_2 = \phi_2(1)$, respectively. In all the cases the energy barriers between the equilibrium angular orientations of the phenyl rings are of the order of k_BT (k_B is the Boltzmann constant) or much less this magnitude thus according to the Boltzmann statistic one may expect large angular amplitudes in their rotational dynamics at room temperature ($T = 300$ K). However, the molecular dynamics aspects appears beyond the scope of

Author's personal copy

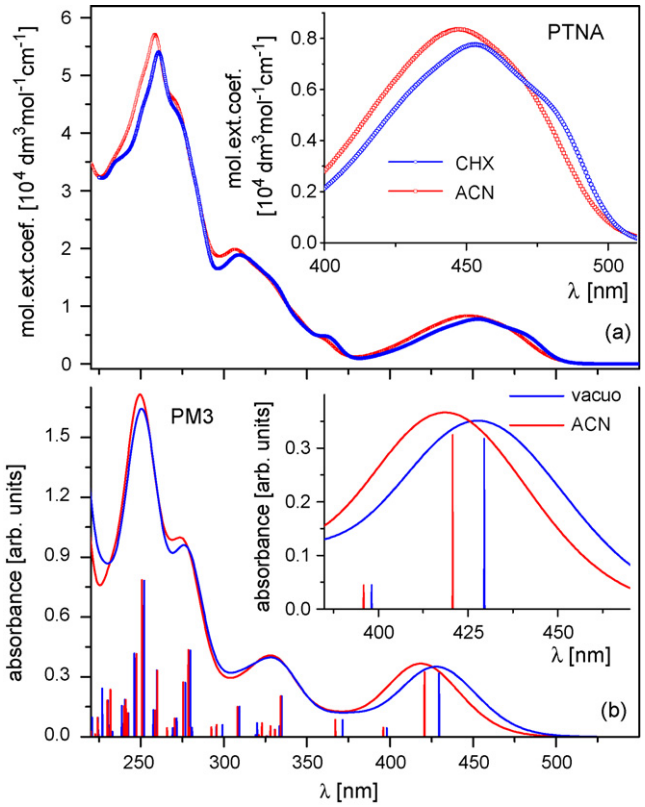

Fig. 2. The optical absorption spectra of PTNA dye. Section (a) shows the measured spectra in CHX (blue color) and ACN (red color) solutions. Section (b) shows the calculated spectra in vacuo (blue color) and in ACN solution (red color); the vertical lines are the oscillator strengths corresponding to the electronic transitions between the ground and excited CI states (represent the spectra calculated at $\Gamma = 0$); the continuous lines simulate the optical absorption spectra by introducing the Gaussian lineshape broadening ($\Gamma = 0.35$ eV). The inserts are the detailed plots in the region of the first absorption band. (For interpretation of the references to color in this figure legend, the reader is referred to the web version of the article.)

the current study and will be published elsewhere. Here we analyze the experimental results within the semiempirical approach being limited by the equilibrium molecular conformations only.

Figs. 2(a) and 3(a) show the optical absorption spectra of the PTNA and DPIPQ dyes measured in CHX and ACN solvents. In the range of 230–600 nm the absorption spectrum of PTNA in CHX solution is characterized by 4–5 absorption bands with the first absorption band centered at about 453 nm and the strongest band at 260 nm. The first absorption band is slightly structured exhibiting several strongly overlapping broad vibronic bands equally spaced by about 1340 cm^{-1}. Similarly DPIPQ in CHX solution is characterized by broad and more evidently structured first absorption band with a maximum at 452 nm and vibronic bands spaced by 1240 cm^{-1}. At higher excitation energies DPIPQ exhibits two strong absorption bands at 295 and 260 nm.

Figs. 2(b) and 3(b) present the calculated optical absorption spectra, where by a blue color there are shown the spectra calculated for the isolated molecules in vacuo. The vertical lines corresponds to the oscillator strengths due to the electronic transitions between the ground (S_o) and excited CI (S_i) states. The continuous lines simulate the optical absorption spectra by introducing the Gaussian lineshape broadening. In such approach the optical density $lg(I_0/I)$ is assumed to be $\propto \sum_{i=1}^{n} \nu_{0i} |\mu_{0i}^{t}|^2 \exp\{-2.773(h\nu - E_{S_i} + E_{S_0})^2/\Gamma^2\}$, where E_{S_o} and E_{S_i} are the energies according to the ground and the excited CI states, $\vec{\mu}_{0i}^{t}$ is the transition dipole moment for the electronic $S_0 \rightarrow S_i$ transition, $\nu_{0i} = (E_{S_i} - E_{S_o})/h$ is corresponding excitation frequency and h is the Planck constant. The superposition is taken over all n CI states with the transition energies that occur in the spectral region subjected to analysis. The empirical parameter Γ has been chosen at the magnitudes of 0.35 eV (0.28 eV) as for PTNA (DPIPQ) in order to obtain the optical absorption spectra similar to the measured ones. Comparing panels (a) and (b) in Fig. 2 or Fig. 3 one can realize that the semiempirical model PM3 quite well reproduces the basic features of the measured spectra. However, the calculated absorption bands are slightly blue shifted with respect to the measured ones. Corresponding wavelength shifts appears in the range of 10–25 nm which depending on the spectral region can be translated to a discrepancy in electronic transition energies in the range of 0.07–0.4 eV.

In the strongly polar solvent, like e.g. ACN, the spectral position of the first optical absorption band of both PTNA and DPIPQ dyes is subjected to a hypsochromic (blue) shift of about 6 nm comparing to the spectral positions revealed in weakly polar CHX solution, see Figs. 2 and 3. This appears to be in contrast with the measured fluorescence spectra which for both dyes are characterized by a bathochromic (red) shift, see Fig. 4(a) and (b) for PTNA and DPIPQ dyes, respectively. In the high and medium polar solvents the photoluminescence spectra are unstructured. However, some vibronic structuring of the photoluminescence bands occurs in weakly polar solvents (like, e.g. CHX) being more evidently seen for PTNA dye [see Fig. 4(a)]. On the other hand, the DPIPQ dyes exhibit much stronger solvatochromic shift indicating substantial magnitude of the dipole moment in the excited state. The absorption and emis-

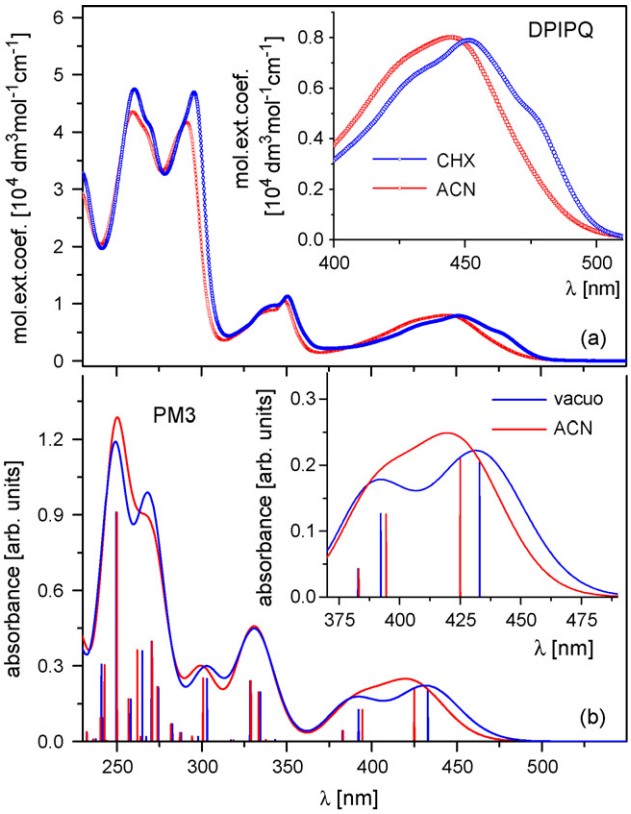

Fig. 3. The optical absorption spectra of DPIPQ dye. Section (a) shows the measured spectra in CHX (blue color) and ACN (red color) solutions. Section (b) shows the calculated spectra in vacuo (blue color) and in ACN solution (red color); the vertical lines are the oscillator strengths corresponding to the electronic transitions between the ground and excited CI states (represent the spectra calculated at $\Gamma = 0$); the continuous lines simulate the optical absorption spectra by introducing the Gaussian lineshape broadening ($\Gamma = 0.28$ eV). The inserts are the detailed plots in the region of the first absorption band. (For interpretation of the references to color in this figure legend, the reader is referred to the web version of the article.)

Author's personal copy

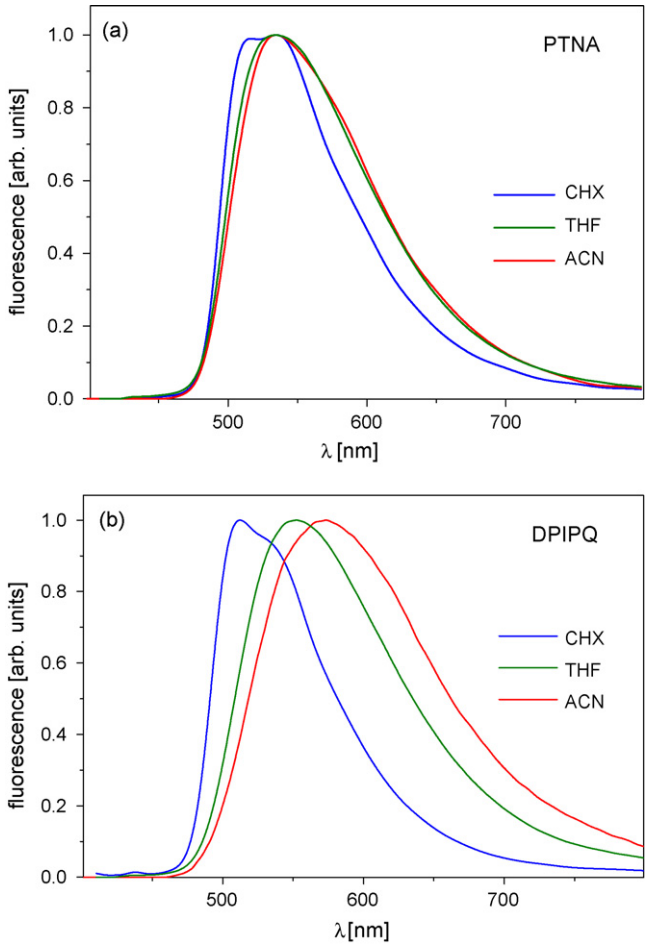

Fig. 4. Steady-state normalized fluorescence spectra of PTNA [(a)] and DPIPQ [(b)] dyes measured in CHX (blue), THF (green) and ACN (red) solutions. (For interpretation of the references to color in this figure legend, the reader is referred to the web version of the article.)

sion maxima of PTNA and DPIPQ obtained in solvents of different polarity are reported in Table 1 together with the measured quantum yield Φ_{fl} and the fluorescence lifetime τ_{fl}. Other photophysical constants such as radiationless (k_{nr}) and radiative (k_{fl}) rate constants have been derived by applying a simple kinetic model of an irreversible excited charge transfer state formation (see e.g. Ref. [37]):

$$k_{nr} = \frac{1-\Phi_{fl}}{\tau_{fl}}, \qquad k_{fl} = \frac{\Phi_{fl}}{\tau_{fl}} \tag{1}$$

whereas the fluorescence transition moment M_{fl} has been evaluated via the radiative rate constant using the relation

$$k_{fl} = \frac{64\pi^4}{3h} n^3 \nu_{fl}^3 |M_{fl}|^2 \tag{2}$$

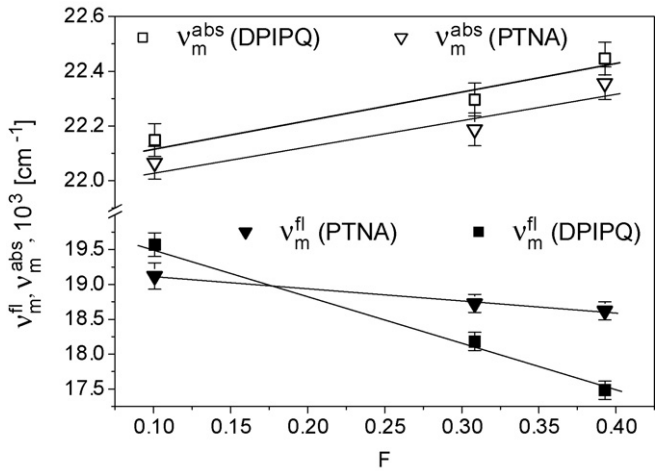

Fig. 5. Solvatochromic plots for PTNA and DPIPQ dyes: optical absorption and fluorescence emission maxima as functions of the solvent polarity parameter F.

where $\nu_{fl} = 1/\lambda_m^{fl}$, n is the solvent refractive index. Both dyes exhibit rather similar values of M_{fl} in all the solvents. While the solvent polarity changes from CHX to ACN the fluorescence moment of PTNA or DPIPQ dyes decreases accordingly about 5% or 15% only. This fact suggests that the electronic structure and molecular conformation of the fluorescent states should not change significantly with the solvent polarity.

We characterize the solvatochromic effect in the term of Lippert–Mataga dielectric polarization model [38,39] which assumes a point dipole situated in the center of the spherical cavity and neglects the solute polarizability in the states involved into the electronic transition. Following this theory the solvent modified spectral positions of the optical absorption ($\nu^{abs} = 1/\lambda^{abs}$) and fluorescence ($\nu^{fl} = 1/\lambda^{fl}$) bands are defined as:

$$\nu^{abs} = \nu_0^{abs} - \frac{2\vec{\mu}_g(\vec{\mu}_e - \vec{\mu}_g)F(\varepsilon, n)}{hca_0^3} \tag{3}$$

$$\nu^{fl} = \nu_0^{fl} - \frac{2\vec{\mu}_e(\vec{\mu}_e - \vec{\mu}_g)F(\varepsilon, n)}{hca_0^3} \tag{4}$$

where

$$F(\varepsilon, n) = \frac{\varepsilon - 1}{2\varepsilon + 1} - \frac{1}{2}\frac{n^2 - 1}{2n^2 + 1} \tag{5}$$

is the solvent polarity function; ν_0^{abs} and ν_0^{fl} are the spectral positions of the absorption and fluorescence maxima in the gas-phase, respectively; c is the light speed in vacuo; a_0 is the effective radius of the Onsager cavity [40]; $\vec{\mu}_g$ and $\vec{\mu}_e$ are the ground and the excited state dipole moments, respectively. Fig. 5 shows the dependences of ν_m^{abs} and ν_m^{fl} vs. the solvent polarity F. The linear character of these plots allows to determine directly the values of $\vec{\mu}_g(\vec{\mu}_e - \vec{\mu}_g)/a_0^3$ and $\vec{\mu}_e(\vec{\mu}_e - \vec{\mu}_g)/a_0^3$ which are collected in Table 2. On the other hand, they can be evaluated having the ground and excited state

Table 1
The photophysical constants of PTNA and DPIPQ dyes obtained in the CHX, THF and ACN solutions. λ_m^{abs} is the absorption maxima, λ_m^{fl} is the fluorescence maxima, Φ_{fl} is the fluorescence quantum yield, τ_{fl} is the fluorescence lifetime, k_{nr} is the radiationless rate constant, k_{fl} is the radiative rate constant and M_{fl} is the fluorescence moment.

Compound	Solvent	λ_m^{abs} [nm]	λ_m^{fl} [nm]	Φ_{fl}	τ_{fl} [ns]	k_{nr} [10^7, s^{-1}]	k_{fl} [10^7, s^{-1}]	M_{fl} [D]
PTNA	CHX	453	523	0.45	18.1	3.1	2.5	1.98
	THF	451	534	0.40	17.3	3.5	2.3	2.01
	ACN	447	537	0.31	18.0	3.8	1.7	1.87
DPIPQ	CHX	452	511	0.410	12.6	4.7	3.3	2.19
	THF	449	550	0.195	12.8	6.3	1.5	1.71
	ACN	446	572	0.092	6.2	14.6	1.5	1.91

Author's personal copy

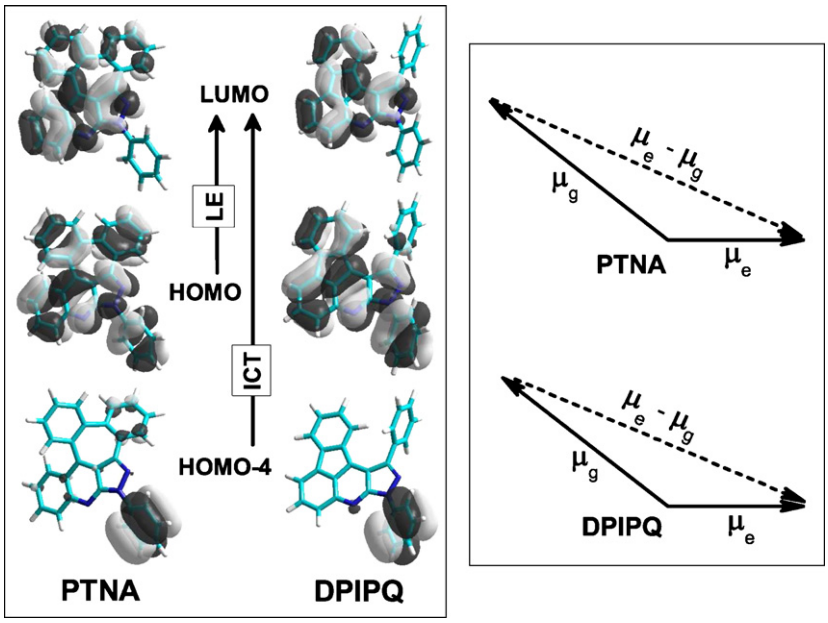

Fig. 6. Electronic transitions in PTNA and DPIPQ dyes. Left panel shows the molecular orbitals HOMO-4, HOMO and LUMO calculated within semiempirical method PM3. Right panel presents the vector diagrams composed of the ground and excited states dipole moments.

dipole moments being calculated within the semiempirical model PM3. A crude parameter of such evaluation is the Onsager cavity radius a_0. Formally, it can be roughly evaluated from the molecular volume. Such a way is frequently applied by many authors, however it indeed does not provide always a correct result, especially if one deals with larger molecules. Thus we will consider it as a flexible model parameter being adjusted in each case in order to provide the best agreement with the experiment. For instance, with the Onsager cavity radius $a_0 = 6.3$ Å, as determined from the molecular volume, one obtains rather poor agreement with experiment (see Table 2). Much better agreement is obtained at smaller cavity radius, e.g. $a_0 = 4.3$ Å. Importantly, that the quantum chemical calculations give for both dyes a proper sign of the magnitudes $\vec{\mu}_g(\vec{\mu}_e - \vec{\mu}_g)/a_0^3$ and $\vec{\mu}_e(\vec{\mu}_e - \vec{\mu}_g)/a_0^3$ which indeed define the slope of solvatochromic shifts and explain, in particular, why the bathochromic (red) shift of the fluorescence spectra is accompanied by the hypsochromic (blue) shift of the absorption spectra. Deeper reason for this lies in specific orientation of the dipole moments $\vec{\mu}_g$ and $\vec{\mu}_e$, see vector diagram in Fig. 6, right panel. One can realize that for both dyes the vector difference $\vec{\mu}_e - \vec{\mu}_g$ appears to be almost parallel to $\vec{\mu}_e$ and nearly antiparallel to $\vec{\mu}_g$. Comparing the calculated and measured magnitudes of $\vec{\mu}_g(\vec{\mu}_e - \vec{\mu}_g)/a_0^3$ one must mention rather good agreement for both dyes. However, with regard to other value $\vec{\mu}_e(\vec{\mu}_e - \vec{\mu}_g)/a_0^3$, which indeed defines the solvatochromic behavior of the fluorescence spectra, the discrepancy between the experiment and theory must be admitted. It is especially strong for DPIPQ dye, for which the experiment suggests much larger dipole moment of the excited fluorescence state ($|\vec{\mu}_e|$) comparing to the one which follows from the semiempirical calculations. It has to be kept in mind that the quantum chemical calculations yield the values of the excited state moments $|\vec{\mu}_e(S_i)|$ which corresponds to the singlet states S_i in the gas phase, not for the solvated phase which are the conditions of the experiments. In the gas-phase the first excited singlet state S_1 of both dyes is composed preferably of HOMO → LUMO transition which according to Fig. 6 (see left panel) can be evidently classified as a local one. Accordingly, the locally excited (LE) state S_1 is characterized by relatively small value of the state dipole moment $|\vec{\mu}_e(S_1)|$, 1.53 and 1.49 D as for PTNA and DPIPQ, respectively. It is also separated by a quite large energy gap from higher energy intramolecular charge transfer (ICT) states with sufficiently larger state dipole moments. Quantum chemical analysis shows that such ICT states indeed exist, the lowest one for DPIPQ (PTNA) corresponds to the excitation energies of about 5.7 eV (5.8 eV), i.e. it is separated from the lowest LE state by the energy gap of about 2.9 eV (3.0 eV). The ICT state in this case is composed mainly of HOMO-4 → LUMO transition (see Fig. 6, left panel) being characterized in DPIPQ (PTNA) by a strong charge transfer from electron-donating group Ph2 (Ph) to electron-accepting phenyl-azafluoranthene (phenyl-azulene) moiety. Corresponding excited states are found to be with a large dipole moments, about 20 D for both dyes. Thereby, in polar solvents the energy of these states considerably lowers thus the energetic closeness should result in an enhanced mixing of the ICT state with the lowest LE state leading to their mutual modification. Corresponding mechanism has been considered earlier (see e.g. Ref. [41,42]). However, to treat this problem properly one should include the solvation energy corrections directly in the Hamiltonian.

Table 2
Slopes of the solvatochromic plots for PTNA and DPIPQ dyes as determined from optical absorption and fluorescence measurements and calculated within the semiempirical model PM3.

Compound		a_o [Å]	$\vec{\mu}_g(\vec{\mu}_e - \vec{\mu}_g)/a_o^3$ [eV]	$\vec{\mu}_e(\vec{\mu}_e - \vec{\mu}_g)/a_o^3$ [eV]
PTNA	Exp.	–	−0.057	0.11
	Calc.	4.3	−0.077	0.043
	Calc.	6.3	−0.025	0.014
DPIPQ	Exp.	–	−0.063	0.409
	Calc.	4.3	−0.068	0.04
	Calc.	6.3	−0.022	0.013

To get an idea how solvation affects the optical absorption spectra the excitation energies have been corrected according to Eq. (3). The results, presented by red color in Fig. 2(b) or Fig. 3(b) for PTNA or DPIPQ, respectively, show again the oscillator strengths corresponding to the electronic transitions (vertical lines) as well as the simulated optical absorption spectra obtained by introducing the Gaussian lineshape broadening (continuous line) with the parameter Γ having for each dye the same magnitude as for the corresponding spectra in vacuo. The spectra have been calculated for

Author's personal copy

the molecules in ACN solution ($F = 0.3928$) and the Onsager radius $a_0 = 4.3$ Å. One may realize that even such simple model quite well reproduces basic features of the solvatochromic behavior.

5. Conclusion

In conclusion we have reported here the measured optical absorption and fluorescence spectra as well as basic photophysical characteristics of newly synthesized PTNA and DPIPQ dyes being representatives of annulated analogues of azafluoranthene and azulene. The spectra have been recorded in the organic solvents of different polarity in order to analyze the change of the electronic structure caused by solvent-modified electron transfer interactions. The experimental results are compared with the quantum chemical calculations performed within the semiempirical method PM3. While the solvent polarity changes from CHX to ACN both dyes exhibit opposite solvatochromic behavior for the optical absorption and fluorescence spectra: the hypsochromic shift of the first absorption band and the bathochromic shift of the fluorescence band. This fact appears to be consistent with the Lippert–Mataga solvatochromic model and is explained by specific orientations of the ground and excited state dipole moments. On the other hand, quantitative evaluations of the solvatochromic shifts give quite well agreement with the experimental data only for the optical absorption spectra of both dyes. In the case of the fluorescence spectra the experiment suggests much larger dipole moment of the excited state comparing to the one which follows from the semiempirical calculations. Corresponding discrepancy is especially strong for DPIPQ dye and is assumed to be related with an enhanced mixing of the lowest LE state with the lowest ICT states due to lowering of their energies in a polar solvent environment. Both dyes reveal substantial quantum yield what may be of interest for the luminescent or electroluminescent applications. Depending on solvent polarity they emit light in green-yellow range of the visible spectra.

References

[1] V.S. Anthonov, K.L. Hohla, Appl. Phys. B 32 (1983) 9.
[2] S. Speiser, N. Shakkour, Appl. Phys. B 38 (1985) 191.
[3] J. Tu, N. Li, Y. Chi, S. Qu, C. Wang, Q. Yuan, X. Li, S. Qiu, Mater. Chem. Phys. 118 (2009) 273.
[4] X.H. Zhang, B.J. Chen, X.Q. Lin, Q.T.Y. Wong, C.S. Lee, H.L. Kwong, Chem. Mater. 13 (2001) 1565.
[5] G. Mao, A. Orita, L. Fenenko, M. Yahiro, C. Adachi, J. Otera, Mater. Chem. Phys. 115 (2009) 378.
[6] J.-A. Cheng, C.H. Chen, H.-P.D. Shieh, Mater. Chem. Phys. 113 (2009) 1003.
[7] E. Gondek, I.V. Kityk, A. Danel, Mater. Chem. Phys. 112 (2008) 301.
[8] E. Gondek, S. Całus, A. Danel, A.V. Kityk, Spectrochim. Acta A 69 (2008) 22.
[9] E. Koścień, J. Sanetra, E. Gondek, B. Jarosz, I.V. Kityk, J. Ebothe, A.V. Kityk, Opt. Commun. 242 (2004) 401.
[10] E. Gondek, A. Danel, B. Kwiecień, J. Nizioł, A.V. Kityk, Mater. Chem. Phys. 119 (2010) 140.
[11] E. Koścień, J. Sanetra, E. Gondek, B. Jarosz, I.V. Kityk, J. Ebothe, A.V. Kityk, Spectrochim. Acta A 61 (2005) 1933.
[12] P. Zhang, B. Tang, W. Tian, B. Yang, M. Li, Mater. Chem. Phys. 119 (2010) 243.
[13] K.S. Danel, A. Wisła, T. Uchacz, ARKIVOC x (2009) 71.
[14] S.I. Khan, A.C. Nimrod, M. Mehrpooya, J.L. Nitiss, L.A. Walker, A.M. Clark, Antimicrob. Agents Chemother. 46 (2002) 1785.
[15] M.P. Cava, K.T. Buck, A.I. DaRocha, J. Am. Chem. Soc. 94 (1972) 5931.
[16] D.L. Boger, C.E. Brotherton, J. Org. Chem. 49 (1984) 4050.
[17] C.F. Koelsch, A.F. Steinhauer, J. Org. Chem. 18 (1953) 1516.
[18] T. Iwakuma, U.S. Patent 2,00,80,206,597 (2008) (Chem. Abstr. 146 (2008) 337907).
[19] Y. Sato, T. Mizoguchi, Y. Kudo, R. Ishida, U.S. Patent 4,367,230 (1981) (Chem. Abstr. 96 (1981) 217867).
[20] A.A. Asselin, L.G. Humber, U.S. Patent 4,171,443 (1979) (Chem. Abstr. 92 (1979) 41918).
[21] J.-P. Chen U.S. Patent 2,00,40,101,711 (2004) (Chem. Abstr. 141 (2004) 14229).
[22] M. Mercep, M. Mesic, D. Pesic, U.S. Patent 7,312,203 (2007) (Chem. Abstr. 140 (2003) 5037).
[23] M. Mercep, M. Mesic, Pesic D U.S. Patent 20,05,049,015 (2005) (Chem. Abstr. 143 (2005) 13341).
[24] H. Dodziuk, Strained Hydrocarbons, Wiley-VCH, Weinheim, 2009.
[25] H.F. Hua, Y.B. Li, H.B. He, Diamond Relat. Mater. 10 (2001) 1818.
[26] N. Fotopoulos, J.P. Xanthakis, Surf. Interface Anal. 39 (2007) 132.
[27] B.W. Jeong, J. Ihm, G.D. Lee, Phys. Rev. B 78 (2008) 165403.
[28] G.D. Lee, C.Z. Wang, E. Yoon, N.M. Hwang, K.M. Ho, Appl. Phys. Lett. 92 (2008) 043104.
[29] K. Suenaga, H. Wakabayashi, M. Koshino, Y. Sato, K. Urita, S. Iijima, Nat. Nanotechnol. 2 (2007) 358.
[30] S. Liu, P. He, H. Wang, J. Shi, M. Gong, Mater. Chem. Phys. 116 (2009) 654.
[31] D. Tomkute-Luksiene, T. Malinauskas, A.S. Sauskaite, V. Getautis a, K. Kazlauskas, P. Vitta, A. Zukauskas, S. Jursenas, J. Photochem. Photobiol. A Chem. 198 (2008) 106.
[32] M. Matschke, R. Beckert, E.U. Würthwein, H. Görls, Synlett 17 (2008) 2633.
[33] I.B. Berlman, Handbook of Fluorescent Spectra of Aromatic Molecules, 2nd ed., Academic Press, New York (NY), 1971, 415.
[34] E. Koścień, J. Sanetra, E. Gondek, A. Danel, A. Wisła, A.V. Kityk, Opt. Commun. 227 (2003) 115.
[35] E. Gondek, E. Koscien, J. Sanetra, A. Danel, A. Wisla, A.V. Kityk, Spectrochim. Acta A 60 (2004) 3101.
[36] S. Calus, E. Gondek, A. Danel, B. Jarosz, A.V. Kityk, Opt. Commun. 268 (2006) 64.
[37] A. Kapturkiewicz, J. Herbich, J. Karpiuk, J. Nowacki, J. Phys. Chem. A 101 (1997) 2332.
[38] E. Lippert, Z. Naturforsch. A10 (1955) 541.
[39] N. Mataga, Y. Kaifu, M. Koizumi, Bull. Chem. Soc. Jpn. 28 (1955) 690.
[40] L. Onsager, J. Am. Chem. Soc. 58 (1936) 1486.
[41] A. Onkelinx, F.C. De Schryver, L. Viaene, M. Van der Auweraer, K. Iwai, M. Yamamoto, M. Ichikawa, H. Masuhara, M. Maus, W. Rettig, J. Am. Chem. Soc. 118 (1996) 2892.
[42] M. Maus, W. Rettig, S. Depaemelaere, A. Onkelinx, F.C. De Schryver, K. Iwai, Chem. Phys. Lett. 292 (1998) 115.